Journal of Undergraduate Research

Volume 6, Issue 7 - May June 2005

2D SAR Imaging for Bandlimited Data

William Roberts and Jian Li

ABSTRACT

SAR (Synthetic Aperture Radar) data, due to radar hardware or cost limitations, is often bandlimited. Traditional FFT (Fast Fourier Transform) methods for image reconstruction can lead to severe sidelobes that cause confusion in the scene. In this paper, the CLEAN method, an iterative deconvolution procedure, is applied to the case of bandlimited SAR data in hopes of suppressing the sidelobes. The ability of CLEAN to improve image quality will be demonstrated by applying the method to data sets (collected over a variety of bandwidths) modeling a backhoe tractor.

INTRODUCTION

Synthetic Aperture Radar (SAR) provides a means of modeling the electromagnetic reflectivity of an object or scene, and thus effectively providing knowledge of the object's shape and material composition. The quality of the image depends on the quality and the quantity of data collected by the radar. If the data is flawed or incomplete, the image will not be clear. An array of complex values representing the discrete frequency Fourier data of a backhoe tractor was obtained from DARPA and the Air Force Research Laboratory. The data was collected on a polar grid using a SAR device. The challenge presented was to reconstruct the original image, the backhoe, using any variety of methods, but by using data covering only a limited bandwidth. In other words, this project seeks to reduce the cost and boost the efficiency of SAR imaging; less data must be collected in order to reproduce a coherent image. The chosen algorithms for image reconstruction include the fast Fourier transform (FFT) and CLEAN methods. FFT procedures, though computationally efficient, suffer from high sidelobe effects and poor accuracy. Sidelobes are those frequencies containing power that are not present in the original signal; they are an undesirable effect that can cause confusion in the image [1]. To somewhat lessen the effect created by sidelobes, a windowing function was applied to the data. In addition, CLEAN methods, an iterative deconvolution procedure, were proposed to further reduce sidelobe impact. In this paper, the effectiveness of these methods for SAR imaging at a reduced bandwidth will be systematically considered.

PROBLEM FORMULATION

Synthetic Aperture Radar (SAR) is a system that emits and receives frequency-modulated (FM) continuous beams of microwave intensity. The radar device transmits a chirp signal, one whose frequency changes linearly from a

low value to some high value, from a side aimed antenna. Chirp signals serve to raise the transmission power while maintaining a constant bandwidth [2]. Transmission occurs in the range direction, orthogonal to the radar′s path. In contrast, the term cross range, or azimuth, refers to a direction parallel to the path of the radar. Data collection was performed using the spotlight mode, which ensures finer resolution over smaller areas than strip-mapping techniques [3]. As the name suggests, for spotlight mode the radar′s antenna is turned at each look-angle to ‟spotlight″ a specific, single target. The set of returned signals, known as the phase history, are demodulated and processed to produce an image modeling the electromagnetic reflectivity of the ground. SAR imaging presents several distinct advantages over optical and infrared techniques, including its immunity to lighting and weather conditions.

The radar device, after transmission, yields an array of complex terms: the phase history of the scene. However, as SAR is able only to cover a limited range of the scene′s spatial frequency, the resulting inverse Fourier transform of the data will be incomplete. The resolution of the final image depends on the bandwidth, the extent of the frequency information attained. Bandwidth could be limited by cost constraints or simply by the complexity of the radar device.

Let F(_) represent the frequency data of the object from a single observation angle. The frequency information attained by the SAR can be modeled as:

$$G(\omega) = H(\omega)F(\omega)$$

where

$$H(\omega) = \begin{cases} 1 & \text{if } f_c - 0.5f_b < f < f_c + 0.5f_b; \\ 0 & else \end{cases}$$

defines the frequency limits, with f c representing the center frequency of the radar and f b representing the bandwidth.

By duality, multiplication in the frequency domain equates to convolution in the time domain:

$$g(x) = h(x) * f(x)$$

where * denotes the convolution operator. It can then be easily shown that

$$\begin{aligned} h(x) &= F^{-1}[H(\omega)] \\ &= \frac{f_b}{2\pi} e^{j2\pi f_c t} \text{sinc}[\frac{f_b}{2}t]. \end{aligned}$$

Thus, limiting the bandwidth of the frequency information is equivalent to filtering the image by a sinc function.

So, instead of appearing as an impulse, target points in the scene will appear as sinc waves, which lend to sidelobe effects and poor resolution. Increasing the bandwidth serves to narrow the main lobe of the sinc function, improving resolution. As explained, one should seek to recreate a coherent image using as little bandwidth as possible.

SPECTRAL ESTIMATION ALGORITHMS

The following provides a brief explanation of the fast Fourier transform (FFT) and CLEAN algorithms for a 1-D discrete time data sequence x(n).

A. FFT

The radix-2 FFT algorithm, first described by Cooley and Tukey [4], efficiently computes the discrete Fourier transform (DFT) using a divide and conquer approach. The inverse DFT of an array of complex spectral data X[k] is given by

$$x[n] = \frac{1}{N}\sum_{k=0}^{N-1} X[k]e^{j\frac{2\pi kn}{N}} \quad n = 0, 1, 2, ..., N-1 \tag{6}$$

where x[n] is a finite signal and N (constrained to be a power of two) represents its length. The formula is then decomposed to model the signal over its even and odd indexed values:

$$\begin{aligned} x[n] &= \text{IDFT}\{X[k]\} && (7)\\ &= \frac{1}{N}\sum_{k=0}^{N-1} X[k]e^{j\frac{2\pi}{N}kn} && (8)\\ &= \frac{1}{N}\left[X[0]e^{j(0)} + X[2]e^{j\frac{2\pi}{N}2n} + ... + X[N-2]e^{j\frac{2\pi}{N}n(n-2)}\right] + \\ &\quad \frac{1}{N}\left[X[1]e^{j\frac{2\pi}{N}n} + X[3]e^{j\frac{2\pi}{N}3n} + ... + X[N-1]e^{j\frac{2\pi}{N}n(n-1)}\right] && (9)\\ &= \frac{1}{N}\sum_{k=0}^{\frac{N}{2}-1} X[2k]e^{j\frac{2\pi}{N}n(2k)} + \frac{1}{N}\sum_{k=0}^{\frac{N}{2}-1} X[2k+1]e^{j\frac{2\pi}{N}n(2k+1)}. && (10) \end{aligned}$$

Upon rearranging, the final result is obtained

$$\begin{aligned} x[n] &= \frac{1}{N}\sum_{k=0}^{\frac{N}{2}-1} X[2k]e^{\frac{2\pi}{N}n(2k)} + (\frac{1}{N})e^{j\frac{2\pi}{N}n}\sum_{k=0}^{\frac{N}{2}-1} X[2k+1]e^{j\frac{2\pi}{N}n(2k)} && (11)\\ &= \text{IDFT}_{\frac{N}{2}}\{X[2k]\} + (e^{jn\frac{2\pi}{N}})\text{IDFT}_{\frac{N}{2}}\{X[2k+1]\}. && (12) \end{aligned}$$

The complex summations can thus be recursively broken down until the length of each IDFT is two. The calculations then become trivial:

$$x_2[0] = X_2[0] + X_2[1] \quad (13)$$

$$x_2[1] = X_2[0] - X_2[1]. \quad (14)$$

B. CLEAN

The CLEAN algorithm, originally presented by Högbom for use in radio astronomy, is an iterative deconvolution procedure for the removal of unwanted sidelobes [5], [6]. Let the Fourier data of the object be represented by _(k). The measurements are weighted according to the user defined function _(k). The image formed by the observations is known as the "dirty map" (DM):

$$\mathrm{DM} = \mathrm{IFFT}\{\psi(k) \cdot \phi(k)\} \quad (15)$$

for a set of K observations. The "dirty beam" (DB) will be defined as the inverse Fourier transform of the weight function:

$$\mathrm{DB} = \mathrm{IFFT}\{\phi(k)\}. \quad (16)$$

The maximum points of correlation between the DB and the DM will determine the locations of the real data:

$$\mathrm{DM} * \mathrm{DB} = \mathrm{IFFT}\{\psi(k) \cdot \phi(k) \cdot \phi(k)\}. \quad (17)$$

For simplification, we will choose to weight the measured points as unity (and all others to zero). Thus, the correlation function in (17) becomes simply the DM. The CLEAN algorithm is defined as follows. First, the point of maximum zero deflection is located on the dirty map. A dirty beam pattern, normalized to some loop gain, _, and centered at this maximum point, is subtracted out from the dirty map. Ideally, the loop gain should be infinitely small. However, little improvement is noticed for _ less than 0.5, although a longer runtime does result due to the increased number of iterations [3]. The iterations are repeated until the remaining signal is no longer significant. Lastly, the removed signals are returned to a clean map through convolution with a clean beam, typically a Gaussian. The small sidelobes of the clean beam serve to weigh down the higher frequency, more uncertain terms. When excessive noise is present in the data, CLEAN methods can yield little improvement in overall sidelobe reduction. In that case, CLEAN would be unable to differentiate between real data and their noise elements [5].

NUMERICAL EXAMPLES

A 3-D representation of the backhoe tractor can be seen in Figure 1(a).

Fig. 1. (a) 3-D CAD model of the target.

Figure 2 displays the inverse FFT images collected at a 0 degree elevation and over a 110 degree azimuth slice. In Figure 2(a), the bandwidth of the spectral data was only 500 MHz, and a window was not applied to the data. As evidenced, the severe sidelobes plaguing the image create a great deal of confusion. When a window is applied to the data in Figure 2(b), most of the vertical sidelobes are reduced. However, many of the target's features remain smeared and indiscernible. As the bandwidth is gradually increased, the impact of all sidelobes is lessened and the features become better resolved.

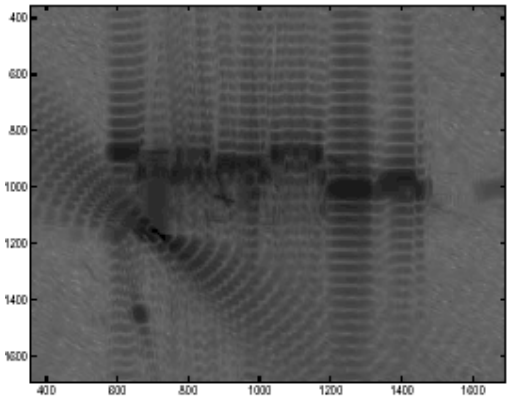

Figure 2. (a) FFT with 0.5 GHz BW

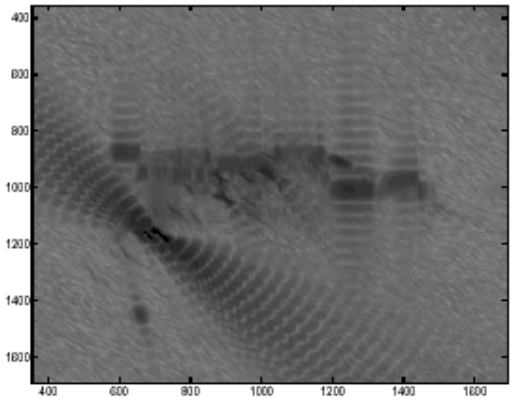

Figure 2. (b) WFFT with 0.5 GHz BW

For Figures 2(c) and 2(d), the bandwidth was increased to 1.0 GHz.

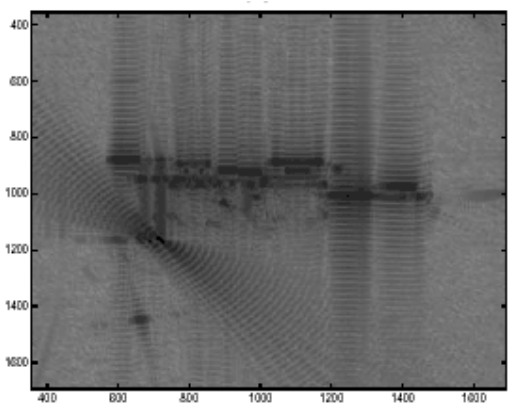

Figure 2. (c) FFT with 1.0 GHz BW

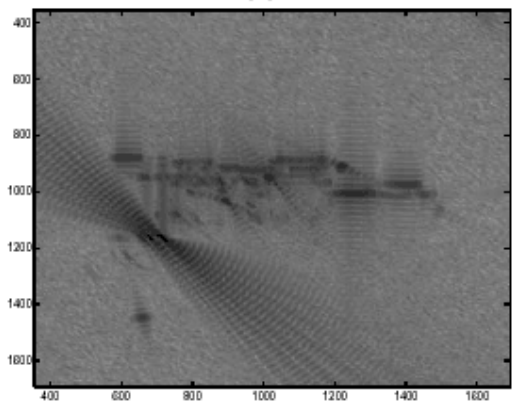

Figure 2. (d) WFFT with 1.0 GHz BW

For Figure 2(e), the bandwidth was raised to 4.0 GHz and a window was not applied to the data. In Figure 2(f), the spectral data was collected over 4 GHz of bandwidth and was subjected to a window. Although the sidelobes are still somewhat apparent, the line features of the target are well defined.

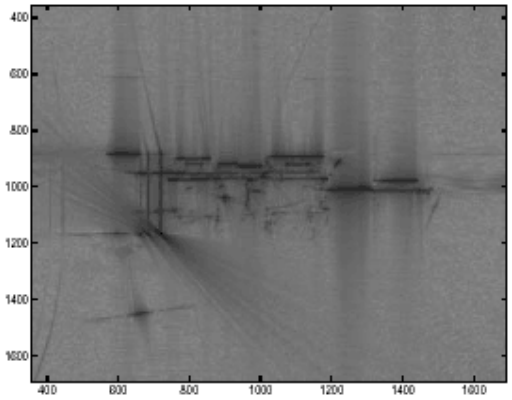

Figure 2. (e) FFT with 4.0 GHz BW

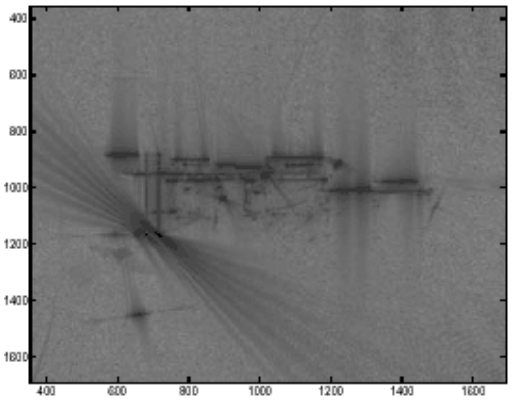

Figure 2. (f) WFFT with 4.0 GHz BW

The images produced using the CLEAN algorithm are shown in Figure 3. For Figure 3(a) and Figure 3(b), the bandwidth of the data was limited to 500 MHz and a loop gain of 0.5 and 1.0 were used, respectively. As evidenced, CLEAN has successfully removed all sidelobes and dramatically improved the resolution of these SAR images for this limited bandwidth case. However, the disadvantage of this algorithm is also evident. CLEAN has misinterpreted several line features of the image into a series of dots. These discontinuities arise when the FFT image is so smeared that CLEAN cannot accurately detect the location of the line features. As the bandwidth is increased, the line features of the object become progressively more continuous. This result should be expected, as the sidelobes are being reduced and the CLEAN algorithm can thus better differentiate the real data.

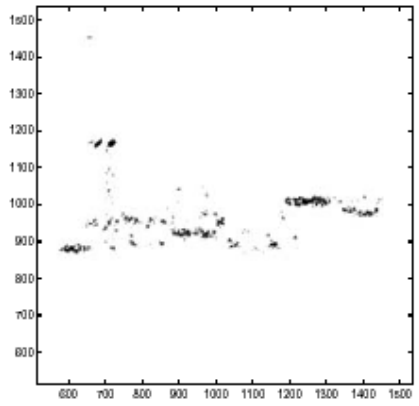

Figure 3. (a) CLEAN (_=0.5, BW=0.5 GHz)

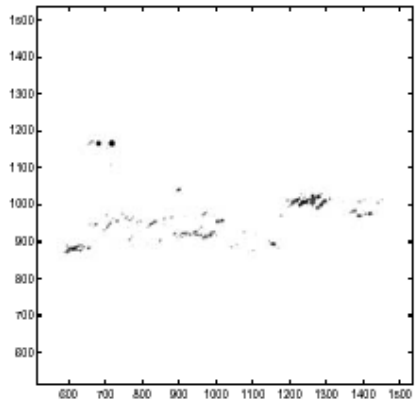

Figure 3. (b) CLEAN (_=1.0, BW=0.5 GHz)

For Figures 3(c) and 3(d), the bandwidth was increased to 1.0 GHz.

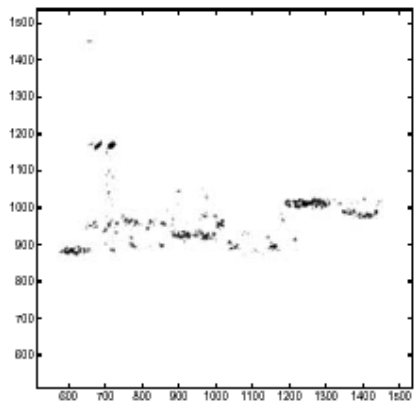

Figure 3. (c) CLEAN (_=0.5, BW=1.0 GHz)

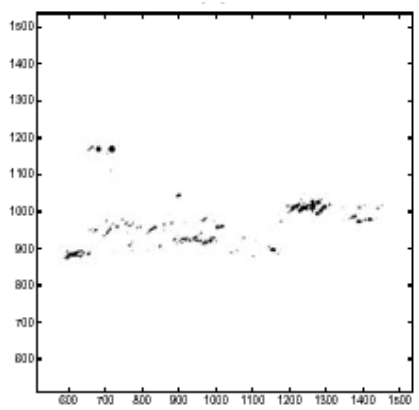

Figure 3. (d) CLEAN (_=1.0, BW=1.0 GHz)

In Figure 3(e) and Figure 3(f), a bandwidth of 2.0 GHz was used with a loop gain 0.5 and 1.0, respectively. The resolution of Figure 3(e) seems comparable to that of Figure 2(f), which was obtained at twice the bandwidth of the CLEAN image.

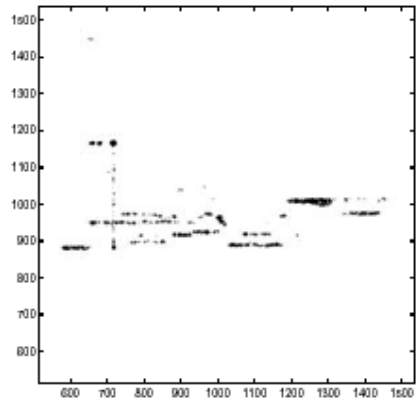

Figure 3. (c) CLEAN (_=0.5, BW=2.0 GHz)

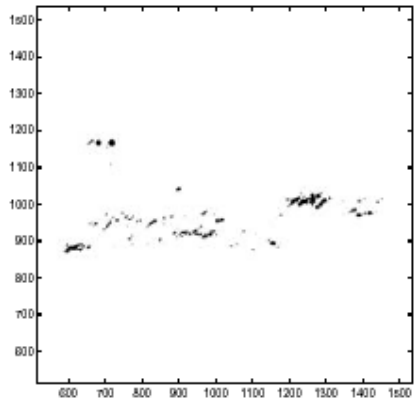

Figure 3. (d) CLEAN (_=1.0, BW=2.0 GHz)

The results in this section also illustrate the effects of altering the value of the loop gain. As mentioned, typically

a value of 0.5 for _ will produce the best results without dramatically increasing the runtime of the algorithm. When _ was set at 1.0 for Figure 3(b), Figure 3(d), and Figure 3(f), the images appear to have lost some data points from the images that used a loop gain of 0.5. This result should be expected, as the loop gain serves to normalize the dirty beam pattern that will be removed from the dirty map at each iteration of the algorithm.

CONCLUSIONS

As shown, SAR data collected at a reduced bandwidth using proper spectral estimation methods may yet be used to form a coherent image. FFT methods for the more bandlimited case produced an image that was plagued with sidelobes. By windowing the data, the sidelobes were reduced, but the resolution was degraded as well. When the bandwidth was increased, the FFT algorithm produced images with narrower spectral peaks and thus more resolved features. The application of CLEAN proved beneficial for the bandlimited case, as sidelobes were removed and resolution was improved. In addition, lower values of the loop gain _ were shown to better preserve the continuity of line features in the image.

Other more sophisticated methods should also be applied to the limited bandwidth scenario. APES (Amplitude and Phase EStimation) [7] and CAPON [8] are adaptive filtering techniques that have been proven to successfully eliminate sidelobes and to produce high resolution images. These methods would achieve better amplitude estimates than the CLEAN and FFT algorithms used in this experiment. Furthermore, extended adaptive filtering (EAF) techniques have recently been developed for APES and CAPON spectral estimators for the case that the data sets are non-rectangular [9]. Although other methods exist for the missing data case, EXAPES and EXCAPON avoid discarding further data (to achieve rectangular data sets) while preserving good second order statistics. CLEAN is able to improve the quality of SAR images efficiently and without computational complexity, but EXAPES and EXCAPON are the techniques best suited for this limited bandwidth case.

REFERENCES

1. P. Stoica and R. Moses, Introduction to Spectral Analysis. Upper Saddle River, NJ: Prentice Hall, 1997.
2. S. A. Hovanessian, Introduction to Synthetic Array and Imaging Radars. Dedham, MA: Artech House, Inc., 1980.
3. J. Charles V. Jakowatz, D. E. Wahl, P. H. Eichel, D. C. Ghiglia, and P. A. Thompson, Spotlight-Mode Synthetic Aperture Radar: A Signal Processing Approach. Boston, MA: Kluwer Academic Publishers, 1996.
4. J. W. Cooley and J. W. Tukey, "An algorithm for the machine calculation of complex fourier series," Mathematics of Computation, vol. 19, no. 90, pp. 297–301, 1965.
5. J. A. Högbom, "Aperture synthesis with a non-regular distribution of interferometer baselines," Astronomy

and Astrophysics Supplements, vol. 15, pp. 417–426, 1974.

6. U. J. Schwarz, "Mathematical-statistical description of the iterative beam removing technique (Method CLEAN)," Astronomy and Astrophysics, vol. 65, pp. 345–356, 1978.
7. J. Li and P. Stoica, "An adaptive filtering approach to spectral estimation and SAR imaging," IEEE Transactions on Signal Processing, vol. 44, no. 6, pp. 1469–1484, June 1996.
8. J. Capon, "High resolution frequency-wavenumber spectrum analysis," Proceedings of the IEEE, vol. 57, pp. 1408–1418, August 1969.
9. Y. Wang, W. Roberts, and J. Li, "Extended adaptive filtering for wide-angle SAR image formation," IEEE Transactions on Aerospace and Electronics Systems, submitted 2004.

--top--

Back to the *Journal of Undergraduate Research*

College of Liberal Arts and Sciences | University Scholars Program | University of Florida |